J. Engg. Math., 16, 181–195 (1982). 0022–0833/82/02/0181–15 $00.20/0

Transverse buckling of a rotating Timoshenko beam

A. NACHMAN and W. D. LAKIN

Department of Mathematical Sciences, Old Dominion University, Norfolk, VA 23508, U.S.A.

(Received June 12, 1981)

SUMMARY

This work considers a group of problems associated with rotating Timoshenko beams. The beam is not assumed to be hubclamped, i.e. the axis of rotation does not necessarily pass through the beam's clamped end. Cases of physical interest involving off-clamped beams include wobbling rotors, impellor blades, and turbine blades.

For clamped-free boundary conditions, we seek solutions of the governing equations which correspond to transverse buckling. For the rotor, it is known that Euler-Bernoulli beams do not have buckled modes. By contrast, the Timoshenko beam will have an infinite number of buckled modes. In the impellor blade case, both Euler-Bernoulli and Timoshenko beams will have an infinite number of buckled modes. However, the Timoshenko beam will buckle at a lower eigenrotation speed. This is also true for the case of a rotating Timoshenko beam with clamped-clamped boundary conditions, e.g. a turbine blade clamped at both the rim and hub of a rotating platform.

Analytic results for both the clamped-free and clamped-clamped cases are augmented by results obtained from numerical solution of the corresponding boundary value problems.

1. Introduction

This paper is a continuation of our investigations into the effects of rotation and precession on the buckling and vibration of beams [2–6]. Here we confine our attention to the transverse (perpendicular to the plane of rotation) buckling of a Timoshenko beam.

As Figure 1 illustrates, if the rotation axis precesses slightly we are essentially modeling a helicopter blade whose drive shaft is slightly bent or undergoes a modest wobble. This will be seen to correspond quantitatively to $\alpha < \frac{1}{2}$, where $\alpha = R/L$ is a dimensionless parameter occurring in the governing equations.

The more realistic accounting of shear, which the Timoshenko beam model purports to give, manifests itself in a significant manner with respect to the question of transverse (out of the page) buckling when $\alpha < \frac{1}{2}$. In short, the Timoshenko beam equations exhibit an infinite number of buckled modes corresponding to an infinite number of eigenrotation speeds Ω_n. By contrast the Euler-Bernoulli model has *no* transverse buckled states when $\alpha < \frac{1}{2}$ [2, p. 482], in consonance with the fact that the axial load is purely tensile.

This dichotomy is reflected mathematically in a very striking manner. The Timoshenko equation contains a dimensionless 'shear parameter' σ, which, when set to zero, provides the governing equation of the Euler-Bernoulli beam [2, p. 491]. Thus we shall be considering

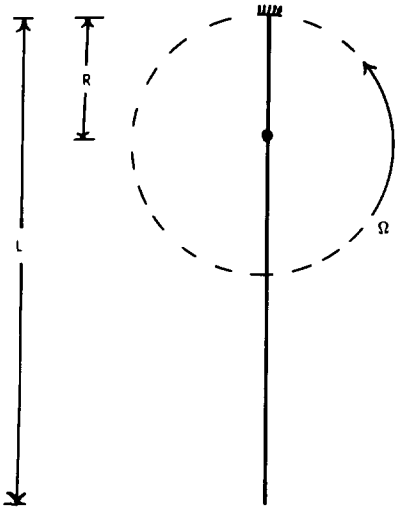

Figure 1. Clamped-free beam of length L rotating in the horizontal plane with constant angular velocity Ω. The clamped end describes a circle of radius R ($0 \leqslant R < L/2$) about the axis of rotation.

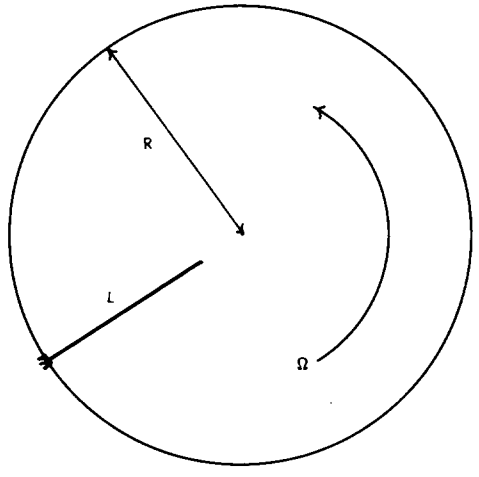

Figure 2. Clamped-free beam of length L attached to the rim of a wheel of radius $R > L$ which rotates in the horizontal plane with constant angular velocity Ω.

an eigenvalue problem which has no eigenvalues when $\sigma = 0$ and an infinite number of eigenvalues as soon as $\sigma > 0$, i.e. when the beam 'becomes' a Timoshenko beam.

When $\alpha \geqslant 1$ we have, as Figure 2 illustrates, a model of an impellor blade. In this case the load will obviously be purely compressive. Thus the existence of an infinite number of transverse buckled states together with their corresponding eigenrotation speeds Ω_n for the Euler-Bernoulli model should come as no surprise [2, p. 491]. The Timoshenko model will likewise have an infinite number of transverse buckled states, but they will occur at lower critical rotation speeds.

When the rotating beam is clamped at the rim and the hub, as in Figure 9, we have a model of a turbine blade. The axial load is compressive near the rim but tensile near the hub. The Euler-Bernoulli model of this situation was considered in [4] and was seen to have an infinite number of buckled states with graphs that all 'wiggled' near the rim. The Timoshenko beam will differ in two respects: the critical rotation speeds will be lower and the eigensolutions will exhibit a nodal structure (i.e. 'wiggle') near the rim and the hub.

2. Governing equations and analysis (clamped-free)

Let $W(x)$ be the deflection of the Timoshenko beam, where x is the distance along the beam measured from the clamped end. Let $\Psi(x)$ denote the slope of the deflection curve when the shearing force is neglected. Then, using the notation of [1], we have

$$EI\Psi_{xx} + kAG(W_x - \Psi) + P(\Psi - W_x) = 0,$$
$$kAG(W_{xx} - \Psi_x) + (P\Psi)_x = 0; \tag{1a, b}$$

$$W(0) = \Psi(0) = 0, \qquad \Psi_x(L) = W_x(L) - \Psi(L) = 0. \tag{2a, b}$$

Here $P(x) = \rho A\Omega^2(L-x)[\frac{1}{2}(L+x) - R]$ (See Figures 1 and 2), k is the Timoshenko constant, A is the cross-sectional area of the beam and $G = 2(1+\nu)E$ is the shear modulus when ν = Poisson's ratio. The beam is clamped (2a) at $x = 0$ and free (2b) at the other end.

A set of dimensionless equations are obtained from the following identifications: $s = x/L$, $\Psi = u(s)$, $W = Lv(s)$, $\mu = \rho AL^4\Omega^2/EI$, $\alpha = R/L$ and $\sigma = 2I(1+\nu)/AL^2k$. Then we have

$$\sigma u'' + (1 - \sigma\mu p(s))(v' - u) = 0, \qquad \sigma\mu(p(s)u)' + (v'' - u') = 0; \tag{3a, b}$$

$$u(0) = v(0) = 0, \qquad u'(1) = v'(1) - u(1) = 0; \tag{4a b}$$

$$p(s) = (1-s)[\tfrac{1}{2}(1+s) - \alpha]. \tag{5}$$

It is clear that (3b) can be integrated from s to 1 and then v' can be eliminated in (3a). This leaves us with the following two point boundary value problem

$$u'' + \mu p(s)[\sigma\mu p(s) - 1]u = 0, \tag{6}$$

$$u(0) = u'(1) = 0. \tag{7a, b}$$

In (6) we regard μ as the eigenvalue and note that $\mu = \mu(\sigma, \alpha)$.

Case 1: $\alpha < \frac{1}{2}$

When $\alpha < \frac{1}{2}$ it is clear that $p(s) \geqslant 0$. Thus when $\sigma = 0$ there can be no positive eigenvalues for (6). It is noted that (6) with $\sigma = 0$ is the Euler-Bernoulli beam [2, p. 491]!

Next we show that for $\sigma > 0$ system (6–7) will have nontrivial solutions. This is one of the results alluded to in the introduction.

We begin with a plausibility argument based on a comparison equation. Note that $p(s) \leqslant \frac{1}{2}(1-\alpha)^2$ for $\alpha < \frac{1}{2}$. Thus consider

$$\begin{aligned} &y'' + \tfrac{1}{2}\mu(1-\alpha)^2[\tfrac{1}{2}\sigma\mu(1-\alpha)^2 - 1]y = 0, \\ &y(0) = y'(1) = 0. \end{aligned} \tag{8}$$

An eigenfunction for (8) is

$$y_n(s) = \sin(\sqrt{\hat{\mu}_n(\sigma\hat{\mu}_n - 1)}\,s) \tag{9}$$

provided

$$\hat{\mu}_n(\sigma\hat{\mu}_n - 1) = (2n+1)^2 \frac{\pi^2}{4}, \tag{10}$$

where $\hat{\mu} = \frac{1}{2}(1-\alpha)^2\mu$. The $\sigma - \hat{\mu}$ response plane tells the whole story. When $\sigma = 0$ there are no eigen-$\hat{\mu}$'s. When $\sigma > 0$, there are an infinite number of eigen-$\hat{\mu}$'s, corresponding to the intersection of horizontal lines with the curves of (10). Solutions of equation (10) are shown in Figure 3.

In order to demonstrate that these same properties are enjoyed by system (6–7) it proves convenient to temporarily regard μ as given and σ as the sought-after eigenvalue. Equation (6) may be written as

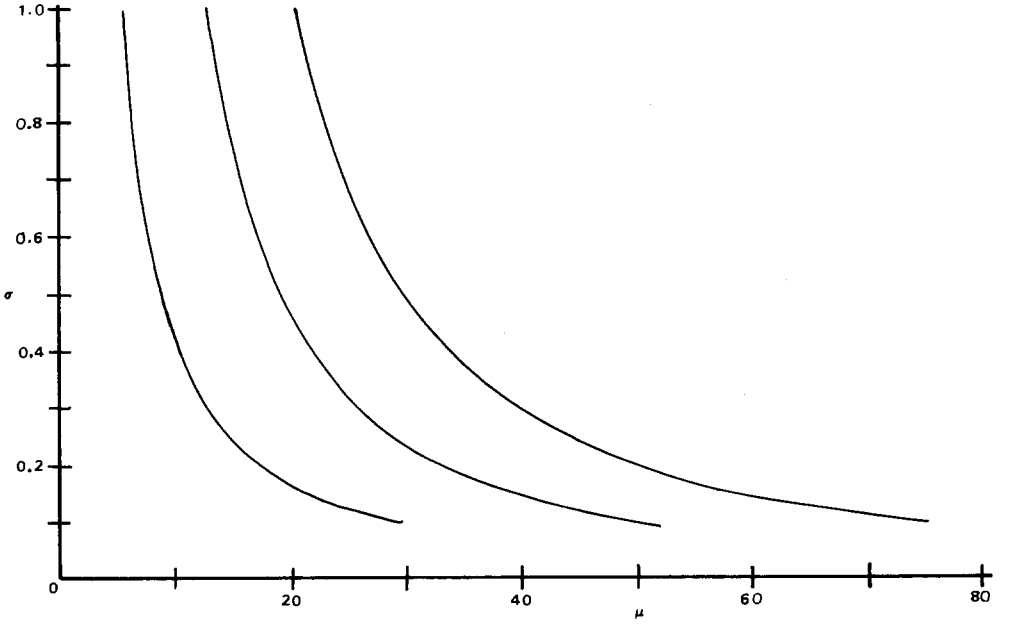

Figure 3. Eigenvalues of the comparison system (8) for $\alpha = 0.1$.

$$u'' - \bar{q}(s)u + \sigma\bar{q}^2(s)u = 0, \tag{$\hat{6}$}$$

where $\bar{q}(s) = \mu p(s)$. Clearly ($\hat{6}$) is in standard Sturm-Liouville form as far as σ is concerned and hence there are an infinite number of eigen-σ's, say σ_n's, for the system ($\hat{6}$–7). This is true for each fixed μ. From the Rayleigh quotient for σ, it is easy to show that $\sigma_n(\mu)$ is a continuous decreasing function of μ with $\sigma_n(0) = \infty$ and $\sigma_n(\infty) = 0$. Thus the picture presented in Figure 3 is qualitatively correct for (6–7).

Lower bounds for $\sigma_n(\mu)$ can easily be provided using the above-mentioned Rayleigh quotient. Of greater utility however, is the following observation. If we return to regarding μ as the eigenvalue for a given σ, then

$$\mu > \frac{2}{(1-\alpha)^2\sigma}. \tag{11}$$

This lower bound is easy to come by – in order for eigenfunctions to exist the coefficient of μ must be positive on some subinterval of $[0, 1]$. Although (11) is a crude lower bound, it is quite useful. Since in practice $\sigma \ll 1$, we see that the first eigenrotation speed is quite large. Equation (11) also shows that the eigenrotation speed is an increasing function of the geometric off-clamping parameter α.

Having obtained the basic properties of $\mu = \mu(\sigma, \alpha)$, we now turn to direct numerical solution of the boundary value problem (6–7) for $\alpha < \frac{1}{2}$. This system was solved using COLSYS [9], a collocation code designed for the solution of nonlinear, multi-point boundary value problems for systems of ordinary differential equations. Solution strategy included appending to (6) the additional scalar differential equation

$$\mu' = 0. \tag{12}$$

Equation (6) is now nonlinear in μ, but this does not cause any computational difficulties. The third-order boundary value problem (6–7, 12) for (μ, u) is now completed by specifying an additional boundary normalization condition

$$u'(0) = 1. \tag{13}$$

Numerical results for the lowest eigenvalue $\mu_0(\sigma, \alpha)$ for $\alpha = 0.0, 0.1, 0.25$ and $\sigma = 0.1$ to 1.0 are given in Table 1. The first two eigenvalues μ_0 and μ_1 are also shown as functions of σ for these three fixed values of α in Figures 4, 5 and 6. To facilitate comparisons, these figures also contain the first two curves defined by (10) [where $p(s)$ is replaced by its upper bound, $\frac{1}{2}(1-\alpha)^2$].

The numerical results confirm the qualitative behavior predicted by (10–11). In particular, for fixed σ, μ is an increasing function of α. Also, $\mu(\sigma, \alpha)$ is large for small σ. For example, the computed value of μ_0 for $\alpha = 0$ and $\sigma = 5 \times 10^{-3}$ is $\mu_0(5 \times 10^{-3}, 0) = 485.77$.

Table 1. Lowest eigenvalue $\mu_0(\sigma, \alpha)$ for the rotating Timoshenko beam with clamped-free boundary conditions and $0 \leqslant \alpha < 1/2$.

σ \ α	0.0	0.1	0.25
0.1	37.03	43.29	57.71
0.2	21.74	25.35	33.62
0.3	16.20	18.87	24.97
0.4	13.25	15.42	20.38
0.5	11.39	13.24	17.48
0.6	10.08	11.73	15.47
0.7	9.12	10.60	13.98
0.8	8.37	9.72	12.82
0.9	7.76	9.02	11.88
1.0	7.26	8.44	11.12

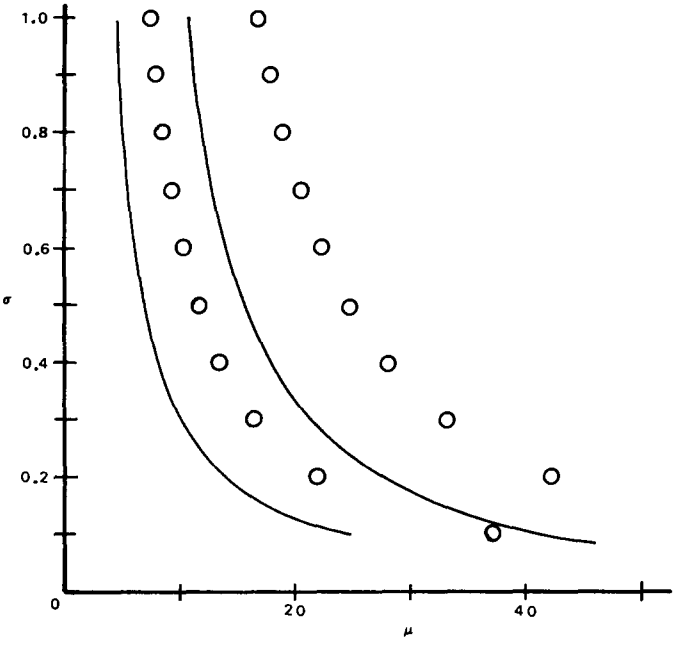

Figure 4. First two eigenvalues for transverse buckling of a rotating Timoshenko beam with clamped-free boundary conditions when $\alpha = 0$. Circled points in the (μ, σ)–plane were obtained by direct numerical solution of (6–7). Solid curves give eigenvalues of the corresponding comparison system (8).

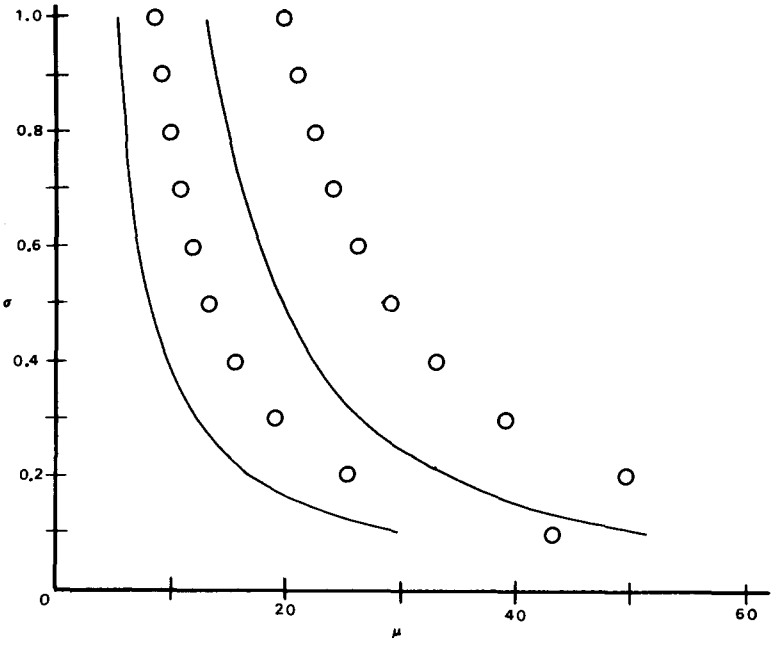

Figure 5. Same caption as Figure 4, but $\alpha = 0.1$.

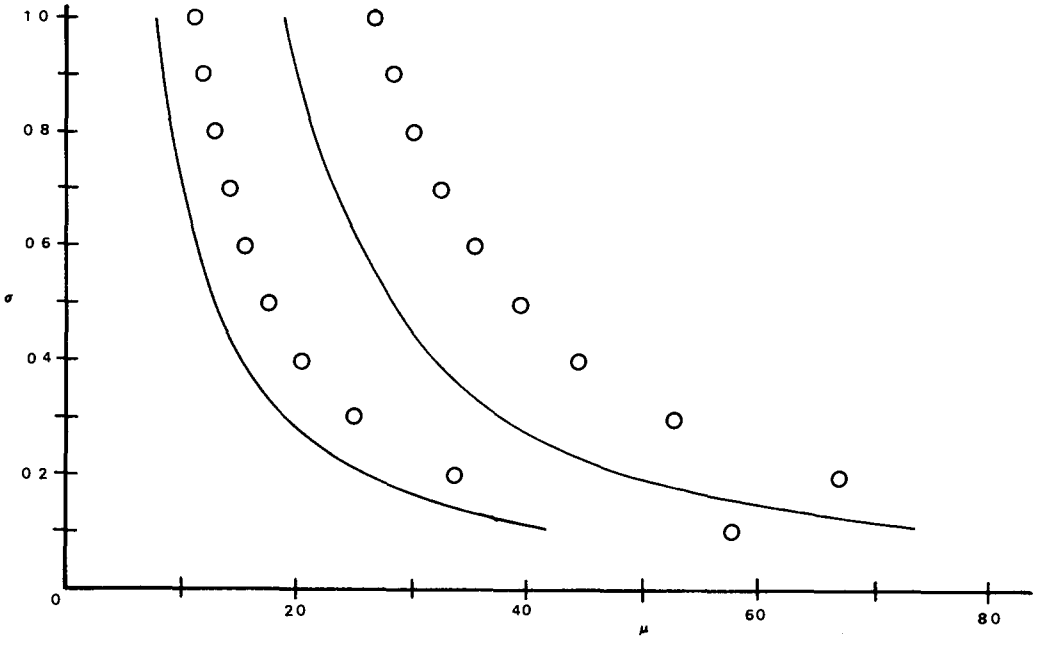

Figure 6. Same caption as Figure 4, but $\alpha = 0.25$.

Case 2: $\alpha > 1$

When $\alpha > 1$ it is clear from (5) that $p(s) \leqslant 0$. Thus (6–7) with $\sigma = 0$ has an infinite number of eigen-μ's. In fact, using the change of variables $t = (s-\alpha)/(1-\alpha)$, we can transform (6–7) (with $\sigma = 0$) into a standard Parabolic Cylinder function equation [8]. The eigen-μ's will then be the roots of

$$W\left(\frac{(1-\alpha)^2}{2}\sqrt{\frac{\mu}{2}}, -\alpha(2\mu)^{1/4}\right)\dot{W}\left(\frac{(1-\alpha)^2}{2}\sqrt{\frac{\mu}{2}}, (\alpha-1)(2\mu)^{1/4}\right)$$

$$= W\left(\frac{(1-\alpha)^2}{2}\sqrt{\frac{\mu}{2}}, \alpha(2\mu)^{1/4}\right)\dot{W}\left(\frac{(1-\alpha)^2}{2}\sqrt{\frac{\mu}{2}}, (1-\alpha)(2\mu)^{1/4}\right), \tag{14}$$

where $(\dot{}) \equiv d/dt$. (See [8] for definition of $W(\alpha, x)$).

Here too we can profitably examine a relevant comparison equation. In this case we have $p(s) \geqslant \frac{1}{2} - \alpha (= p(0))$. Thus, consider

$$y'' + (\tfrac{1}{2}-\alpha)\mu[(\tfrac{1}{2}-\alpha)\sigma\mu - 1]\,y = 0, \qquad y(0) = y'(1) = 0. \tag{15}$$

Once again we have $y_n(s) = \sin(\sqrt{\bar{\mu}(\sigma\bar{\mu}+1)}\,s)$ as an eigenfunction provided $\bar{\mu}_n(\sigma\bar{\mu}_n + 1) = (2n+1)^2\pi^2/4$, where $\bar{\mu}_n = (\alpha - \frac{1}{2})\mu_n$. The $\sigma - \bar{\mu}$ response plane is in Figure 7. The eigen-

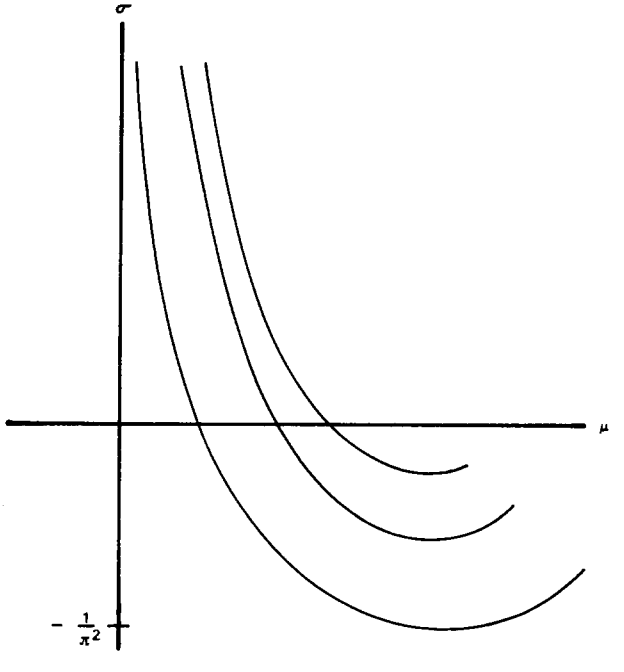

Figure 7. Eigenvalues of the comparison system (15) for $\alpha > 1$.

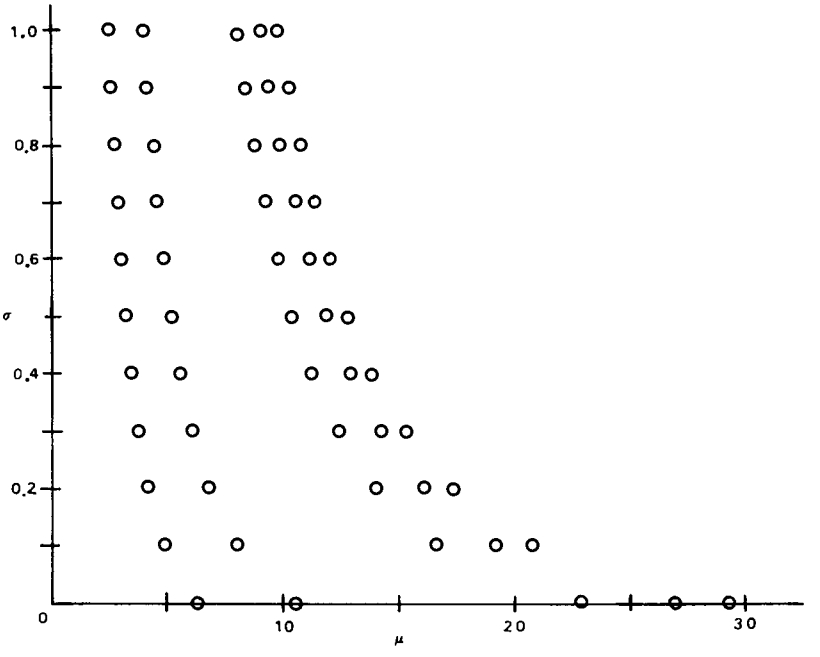

Figure 8. Lowest eigenvalues for transverse buckling of a rotating Timoshenko beam with clamped-free boundary conditions when $\alpha > 1$. Circled points in the (μ, σ)–plane were obtained from direct numerical solution of (6–7). For each σ, the five values shown correspond to (from right to left) $\alpha = 1.025$, 1.05, 1.1, 1.5, and 2.0.

$\bar{\mu}_n$'s are found from the intersection of the curves in Figure 8 with $\sigma =$ constant lines. From this it is clear that $\bar{\mu}_n(\sigma) < \bar{\mu}_n(0)$. If we can show the same to be true for (6–7), then we will have shown that Timoshenko beams buckle at lower rotation speeds than Euler-Bernoulli beams when $\alpha > 1$.

To show that $\mu_n(\sigma) < \mu_n(0)$ for $\sigma > 0$ it suffices to show that $d\mu_n/d\sigma < 0$ for $\sigma > 0$. To do this take $d/d\sigma$ of (6–7). This gives

$$\mu_\sigma'' + \mu^2 p^2 \sigma u_\sigma - \mu p u_\sigma = up(\mu_\sigma - 2\mu\mu_\sigma \sigma p - \mu^2 p), \qquad u_\sigma(0) = u_\sigma'(1) = 0.$$

If μ is an eigenvalue of (6–7), then the Fredholm alternative theorem demands that

$$\int_0^1 u^2 p^3 (\mu_\sigma - 2\mu\mu_\sigma \sigma p - \mu^2 p) ds = 0$$

or

$$\mu_\sigma \int_0^1 u^2 p^3 (1 - 2\mu\sigma p) ds = \mu^2 \int_0^1 p^4 u^2 ds.$$

Recall that $p(s) \leqslant 0$ here and $\sigma > 0$. Q.E.D.

Table 2. Lowest eigenvalue $\mu_0(\sigma, \alpha)$ for the rotating Timoshenko beam with clamped-free boundary conditions and $\alpha > 1$.

σ \ α	1.025	1.05	1.1	1.5	2.0
0.0	29.27	26.81	22.95	10.61	6.33
0.1	20.76	19.18	16.64	8.00	4.83
0.2	17.33	16.05	13.98	6.80	4.13
0.3	15.28	14.18	12.37	6.07	3.69
0.4	13.87	12.88	11.25	5.54	3.38
0.5	12.81	11.90	10.41	5.14	3.14
0.6	11.98	11.14	9.75	4.83	2.95
0.7	11.30	10.51	9.20	4.57	2.79
0.8	10.73	9.98	8.75	4.35	2.66
0.9	10.25	9.53	8.36	4.16	2.54
1.0	9.82	9.14	8.02	3.99	2.44

Results obtained by direct numerical solution of the boundary value problem for $\alpha > 1$ confirm that the Timoshenko beam will buckle at a lower rotation speed than the Euler-Bernoulli beam. Numerical results for the lowest eigenvalue μ_0 for five values of α and σ from 0 to 1 are given in Table 2 and Figure 8.

3. Governing equations and analysis (clamped-clamped)

The only changes necessary to model the turbine blade (Figure 9) are to change $P(x)$ to

$$P(x) = \rho A \Omega^2 \{\tfrac{1}{2} L(R - \tfrac{2}{3}L) + (L - x)[\tfrac{1}{2}(L + x) - R]\}^* \tag{16}$$

and to clamp both ends so that (2b) is replaced by

$$W(L) = \Psi(L) = 0. \tag{17}$$

In this case the dimensionless axial load is

$$\hat{p}(s) = \tfrac{1}{2}(\alpha - \tfrac{2}{3}) + (1 - s)[\tfrac{1}{2}(1 + s) - \alpha]. \tag{18}$$

*Note that $\alpha \geqslant 1$ and $R - L$ is the hub radius.

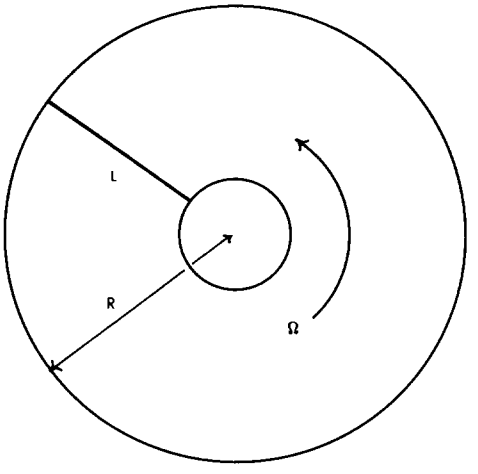

Figure 9. Clamped-clamped beam of length L rotating in the horizontal plane with constant angular velocity.

Note that $\hat{p}(0) < 0$ (compression) and $\hat{p}(1) > 0$ (tension). The governing dimensionless equations are now (3a, b), but with $p(s)$ replaced by $\hat{p}(s)$ and with (4b) replaced by

$$u(1) = v(1) = 0. \tag{19}$$

To analyze this problem integrate (3b) between 0 and s to get

$$\sigma\mu\hat{p}(s)u + v' - u = k = v'(0), \tag{20}$$

where k is, for the moment, unknown. As before, we substitute (20) into (3a) and obtain the boundary value problem

$$u'' + \mu\hat{p}(\sigma\mu\hat{p} - 1)\mu = \frac{k}{\sigma}(\sigma\mu\hat{p} - 1), \tag{21}$$

$$u(0) = u(1) = 0 \tag{22}$$

and

$$\int_0^1 (\sigma\mu\hat{p} - 1)u\,ds = k. \tag{23}$$

Condition (23) comes from integrating (20) between 0 and 1.

System (21–23) is the same sort of unusual eigenvalue problem encountered in [4, bottom of p. 195]. It once again proves convenient to temporarily regard μ as given and σ as the eigenvalue.

To unravel (21–23) we first turn our attention to the following standard Sturm-Liouville system:

$$\phi'' - \hat{q}\phi + \hat{o}\hat{q}^2\phi = 0, \qquad \phi(0) = \phi(1) = 0, \tag{24}$$

where $\hat{q}(s) = \mu\hat{p}(s)$.

There are an infinite number of eigenvalues $\hat{\sigma}_n$ of (24) together with their respective eigenfunctions $\phi_n(s)$.

Consider the following two expansions:

$$u(s) = \Sigma u_n \phi_n(s), \tag{25}$$

$$\frac{k}{\sigma\hat{q}^2}(\sigma\hat{q} - 1) = \Sigma A_n \phi_n(s), \tag{26}$$

where

$$u_n = \int_0^1 \hat{q}^2(s)u(s)\phi_n(s)ds \tag{27}$$

and

$$A_n = \int_0^1 \frac{k}{\sigma}(\sigma\hat{q} - 1)\phi_n(s)ds. \tag{28}$$

Since $\hat{p}(s_0) = 0$ for a unique $s_0 \in (0, 1)$ we see that the left-hand side of (26) does not belong to $L_2^{(0,1)}(\hat{q}^2)$, i.e. the set of functions which are square integrable on (0, 1) with respect to the weight function $\hat{q}^2$. Thus equality in (26) is at best point wise (though in fact uniform on compact subsets not containing s_0) while (25) converges absolutely and uniformly (see [7, p. 168]).

In any event, we have

$$A_n = \int_0^1 (u'' - \hat{q}u + \sigma\hat{q}^2 u)\phi_n ds = (\sigma - \hat{\sigma}_n)\int_0^1 \hat{q}^2 u\phi_n ds = (\sigma - \hat{\sigma}_n)u_n. \tag{29}$$

Thus

$$u(s) = \sum\left(\frac{A_n}{\sigma - \hat{\sigma}_n}\right)\phi_n(s) = \frac{k}{\sigma}\sum\frac{[\int_0^1(\hat{\sigma}q - 1)\phi_n ds]}{\sigma - \hat{\sigma}_n}\phi_n(s) \tag{30}$$

and enforcing (23) results in

$$\frac{1}{\sigma}\sum\frac{[\int_0^1(\sigma\hat{q} - 1)\phi_n ds]^2}{\sigma - \hat{\sigma}_n} = 1. \tag{31}$$

If we call the left-hand side of (31) $F(\sigma)$, then equation (31) may be envisioned as in Figure 10. The desired eigen-σ's of (24) (σ_n's) are given by the intersections of the curves $F(\sigma)$ and the horizontal line at unit height. We also note that as $\hat{\sigma}\hat{q}^2 - \hat{q}$ is positive for $s < s_0$ and near $s = 1$ for sufficiently large $\hat{\sigma}$, the functions $\phi_n(s)$ will always have a nodal structure ('wiggle') for

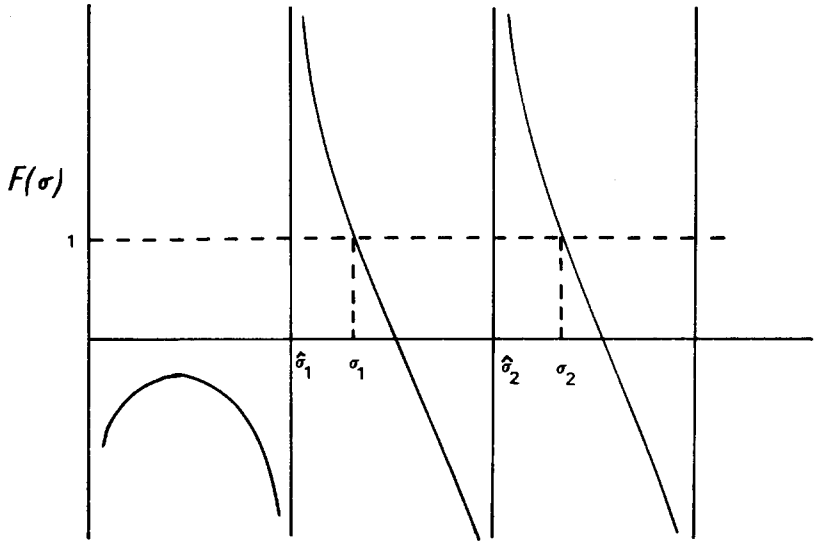

Figure 10. The function $F(\sigma)$ defined by equation (31).

$s < s_0$ and also near $s = 1$ for n sufficiently large. This same behaviour is clearly inherited by $u(s)$ and $v(s)$.

Having shown that (21–23) is, in fact, an eigenvalue problem, we now wish to return to considering μ as the eigenvalue and σ as given. Firstly, we note that the σ–μ plane is essentially the same as in Figure 8. Vertical lines cross the curves and determine the eigenvalues $\mu_n(\sigma, \alpha)$ of (21). Also, the eigenvalue μ does not depend on the value of the constant k in (21) and (23). This is easily shown by substituting the Green's function solution of (21–22) into (23). The resulting eigenvalue relation for $\mu(\sigma, \alpha)$ is independent of k. Hence, k may be prescribed by normalizing the eigenfunctions $u_n(s)$ in some standard way, e.g.

$$\int_0^1 u^2 ds = 1 \quad \text{or} \quad \int_0^1 \hat{q}^2 u^2 ds = 1.$$

Finally, we wish to confirm that, as implied by Figure 8, the lowest buckling eigenvalue $\mu_0(\sigma, \alpha)$ for the clamped-clamped rotating Timoshenko beam is smaller than the corresponding eigenvalue $\mu_0(0, \alpha)$ for the Euler-Bernoulli beam, i.e. the Timoshenko beam buckles at a lower rotation speed. To show this behavior, let $\{\tilde{\mu}_m\}$ $(m = 0, 1, 2, \ldots)$ be the infinite discrete set of special values of μ such that $\hat{\sigma}_1(\tilde{\mu}_m) = 0$, where $\hat{\sigma}_1$ is the lowest eigenvalue of (24) and $\tilde{\mu}_0 < \tilde{\mu}_1 < \ldots$. These special values of μ are related to the Euler-Bernoulli buckling problem. Indeed, by [4], if $\mu_j(0, \alpha)$ is the j-th Euler-Bernoulli buckling eigenvalue, then

$$\tilde{\mu}_j < \mu_j(0, \alpha) < \tilde{\mu}_{j+1}. \quad (j = 0, 1, 2, \ldots).$$

Let $\mu = \mu^* < \tilde{\mu}_0$. There are clearly still an infinite number of positive eigenvalues $\hat{\sigma}_n(\mu^*)$ of (24), i.e. the crossing points of the vertical line $\mu = \mu^*$ with the curves. Also, by Figure 10, for

the Timoshenko beam $\hat{\sigma}_1(\mu^*) < \sigma_1(\mu^*) < \sigma_2(\mu^*)$. Hence, if $\sigma = \sigma_1$ is given, then $\mu^*(\sigma_1, \alpha)$ is an eigenvalue of (21–23) and gives a buckling rotation speed for the Timoshenko beam. As

$$\mu^*(\sigma_1, \alpha) < \tilde{\mu}_0 < \mu_0(0, \alpha),$$

the desired result is shown.

Several interesting problems arise in the numerical solution of the eigenvalue problem for the clamped-clamped rotating Timoshenko beam. These problems stem for the fact that we impose boundary conditions at $s = 0$ and $s = 1$ on $v(s)$ itself while the differential equations (3a, b) involve only v' and v''. Thus, even though the eigenvalues $\mu_n(\sigma, \alpha)$ are independent of the constant k in (23), and k may be fixed by normalizing the eigenfunctions, the system (21–22) cannot be solved independently of the integral constraint on k. It is far simpler in this problem to solve the coupled fourth-order equations (3a, b) for u and v directly, subject to the clamped-clamped boundary conditions. Another approach, which also avoids the integral constraint, is to define $w(s) \equiv v'(s) - u(s)$ and solve the third-order system

$$\sigma\mu'' + (1 - \sigma\mu\hat{p}(s))w = 0, \qquad \sigma\mu(\hat{p}(s)u)' + w' = 0 \tag{32a, b}$$

with the clamped-clamped conditions

$$u(0) = u(1) = 0 \tag{33}$$

and the linked condition

$$w(1) - w(0) = 0. \tag{34}$$

Table 3. Lowest eigenvalue $\mu_0(\sigma, \alpha)$ for the rotating Timoshenko beam with clamped-clamped boundary conditions.

σ \ α	1.025	1.05	1.1	1.5	2.0
0.1	119.85	114.84	105.95	65.02	43.67
0.2	76.27	73.07	67.39	41.31	27.73
0.3	59.59	57.08	52.64	32.26	21.65
0.4	50.37	48.25	44.50	27.26	18.30
0.5	44.37	42.50	39.19	24.01	16.12
0.6	40.08	38.40	35.40	21.69	14.56
0.7	36.82	35.28	32.53	19.92	13.37
0.8	34.24	32.80	30.25	18.53	12.43
0.9	32.14	30.79	28.39	17.39	11.67
1.0	30.38	29.10	26.83	16.43	11.03

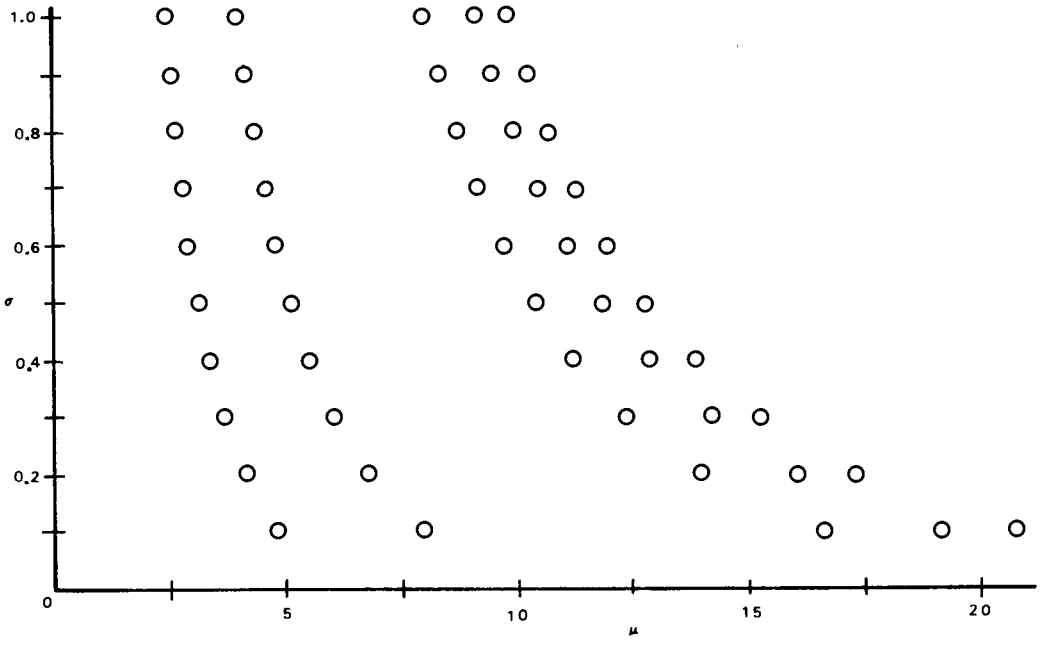

Figure 11. Lowest eigenvalues for transverse buckling of a rotating Timoshenko beam with clamped-clamped boundary conditions. Circled points in the (μ, σ)–plane were obtained by direct numerical solution of (3), (4a), and (19). For each σ, the five values shown correspond to (from right to left) $\alpha = 1.025, 1.05, 1.1, 1.5$, and 2.0.

Equation (34) is obtained by integrating equation (3a) between zero and one and using (33).

Results for the lowest buckling eigenvalue $\mu_0(\sigma, \alpha)$ for five values of $\alpha > 1$ and σ from 0.1 to 1.0 are given in Table 3 and Figure 11. Comparison of the present numerical results with [4] confirms that if $\sigma > 0, \mu_0(\sigma, \alpha) < \mu_0(0, \alpha)$.

References

[1] S. Timoshenko, D. H. Young and W. Weaver, *Vibration problems in engineering*, 4th ed., John Wiley & Sons, 433.

[2] W. D. Lakin and A. Nachman, Unstable vibrations and buckling of rotating flexible rods, *Quart. Appl. Math.* 35 (1978) 479–493.

[3] W. D. Lakin, Vibrations of a rotating flexible rod clamped off the axis of rotation, *J. Eng. Math.* 10 (1976) 313–321.

[4] W. D. Lakin, R. Mathon and A. Nachman, Buckling and vibration of a rotating spoke, *J. Eng. Math.* 12 (1978) 193–206.

[5] W. D. Lakin and A. Nachman, Vibration and buckling of rotating flexible rods at transitional parameter values, *J. Eng. Math.* 13 (1979) 339–346.

[6] S. S. Antman and A. Nachman, Large buckled states of rotating rods, *Nonlinear Analysis, Theory, Methods and Appl.* 4 (1980) 303–327.

[7] H. F. Weinberger, *A first course in partial differential equations with complex variables and transform methods*, Blaisdell Publ., 1965.

[8] M. Abramowitz and I. A. Stegun, *Handbook of mathematical functions*, Dover Publ., New York, 1965.

[9] U. Ascher, J. Christiansen, and R. D. Russell, COLSYS – A collocation code for boundary-value problems , in *Notes on Computer Science* eds. G. Goos and J. Hartmanis, no. 76, Codes for Boundary-Value Problems in Ordinary Differential Equations, Springer-Verlag, (1978) 164–185.